Peer review status: This is a non-peer-reviewed preprint submitted to EarthArXiv

AI-assisted identification of stromatoporoids

David Rodríguez González[1], Consuelo Sendino[2], Stephen Kershaw[2,3], Inés Victoria Rodríguez[1]

[1] Computación Avanzada y eCiencia, Instituto de Física de Cantabria, Avda. de los Castros s/n, 39005 Santander (Cantabria), Spain
[2]Science Group, Natural History Museum, Cromwell Road, London, SW7 5BD, UK [3]Department of Life Sciences, Brunel University London, Uxbridge, UB8 3PH, UK

Corresponding author: Consuelo Sendino
Email: c.sendino-lara@nhm.ac.uk

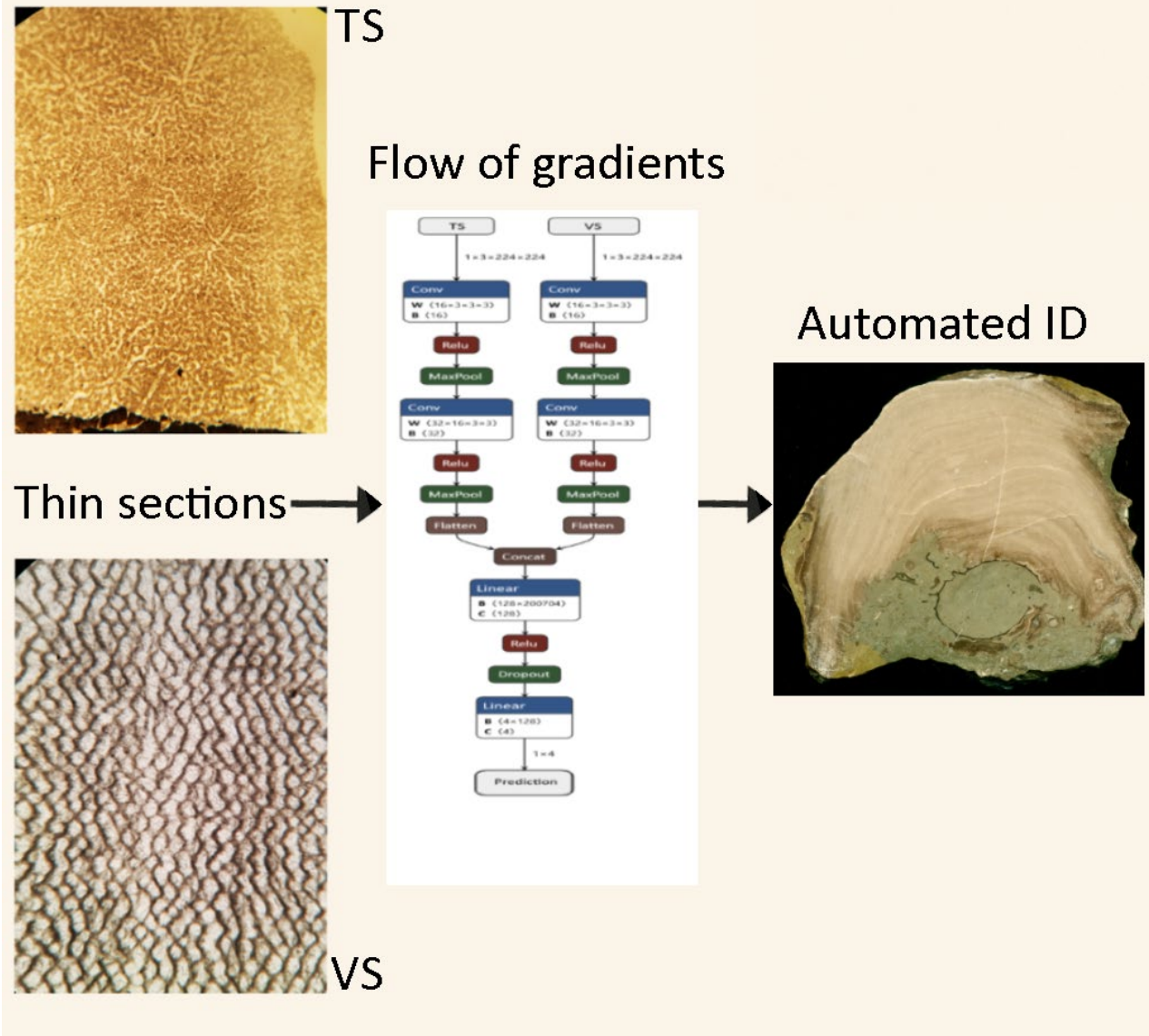

Workflow for automated identification based on stromatoporoid thin sections

ABSTRACT
Stromatoporoid sponge fossils were major diverse reef-builders in the Palaeozoic Era; their taxonomic identification relies on thin sections examined under transmitted light microscopy, where vertical and transverse skeletal elements reveal diagnostic architectural features that vary with taxa. These elements typically appear darker than the cement-filled internal spaces, allowing stromatoporoid taxa to be distinguished. However, stromatoporoid architecture is variable, so that judgement of identification is not always unequivocal. Therefore, this study investigates the application of artificial intelligence (AI) to automate stromatoporoid identification, introducing a novel approach to streamline and standardize palaeontological taxonomy. For the first time, both vertical and transverse sections have been simultaneously analysed and integrated into an automated framework. High-resolution images of thin sections from four well-established Silurian genera, collected from the West Midlands and Shropshire counties, UK, were used to train supervised machine learning models. The images, captured using plane-polarised transmitted light microscopy on thin sections, were digitally enhanced to increase contrast and eliminate background noise, ensuring that only skeletal features were used to inform the models. Despite variations in fossil preservation, section orientation, and image quality, the AI models achieved classification accuracies of up to 96%. This demonstrates that stromatoporoid skeletal architecture is highly amenable to automated analysis, even under suboptimal conditions. The results represent a significant step forward in the application of AI to palaeontology, reducing reliance on manual identification and accelerating the classification process. Ultimately, this approach lays the groundwork for fully automated taxonomic workflows that improve research efficiency and accessibility.

Key words: stromatoporoid, thin section microscopy, AI, machine learning, taxonomy

Introduction and aims

The application of machine learning (ML) techniques to fossil identification is still in its early stages, with significant progress emerging only in the 21st century, primarily in the classification of microfossils (see Yu et al., 2024, for a recent review). These advances have demonstrated the potential of ML to handle complex visual data and extract diagnostic features with high accuracy. However, no attempts have yet been made to apply artificial intelligence (AI) algorithms to the identification of fossil hypercalcified sponges, organisms characterized by the presence of a secondary calcified skeleton, often studied through multiple types of thin section orientations.

Five morphologies, commonly referred to as grades of organisation, of hypercalcified sponges are recognized: archaeocyaths, stromatoporoids, chaetetids, sphinctozoans, and inozoans. Although there is some variation between grades, in the great majority of cases each displays distinctive skeletal architectures; these have been the subject of systematic study for nearly two centuries. Identification is traditionally based on the analysis of thin sections under transmitted light microscopy. There are two types of thin section views: vertical sections, cut perpendicular to the growth surface, and transverse sections, cut parallel to it. In these preparations, the skeletal material typically appears darker than the cement-filled voids that

permeate the structure, allowing researchers to distinguish structural arrangements in both vertical and transverse orientations. The complementary use of vertical and transverse thin sections enables accurate reconstruction of the sponge's three-dimensional skeletal framework (e.g., Huang et al., 2024, fig. 4, for stromatoporoids) and supports accurate taxonomic classification. Although the skeletal structure is inherently three-dimensional, conventional taxonomy relies on the complementary use of vertical and transverse thin sections to capture the necessary morphological variation. The strong visual contrast in colour density between skeletal elements and cement that fills the empty space presents an ideal opportunity for automated, image-based analysis. Although image-analysis software has been applied to stromatoporoids (Wolniewicz, 2010), AI systems hold considerable promise for advancing fossil classification. AI systems can learn complex visual patterns, adapt to variability in preservation and imaging conditions, and scale efficiently across large datasets, capabilities that traditional methods lack.

As a first step toward AI-assisted identification of hypercalcified sponges, this study focuses on stromatoporoids, a group distinguished by well-defined vertical and lateral skeletal elements composed of darker calcium carbonate, with transparent cement-filled voids. These architectural features produce clear contrasts in thin section images, allowing experienced researchers to identify taxa through years of visual training and reference to extensive literature. Stromatoporoids exhibit considerable morphological variation, making them ideal candidates for initial testing of AI-driven taxonomic tools.

The primary objective of this study is to evaluate the feasibility of using AI to identify a limited number of stromatoporoid taxa based on thin section images. Uniquely, this approach integrates both vertical and transverse sections in the training and analysis pipeline, reflecting how taxonomists traditionally interpret these fossils in two dimensions to infer three-dimensional structure. This dual-orientation input marks a novel advance in automated fossil identification, enhancing the model's capacity to detect diagnostic patterns across orientations and represents a novel advance in fossil classification.

Beyond its immediate application, this project has broad potential across multiple domains. In research, AI offers a scalable solution to accelerate and standardise taxonomic classification, and reduce human error. This is particularly valuable for processing large datasets in stratigraphic, palaeoenvironmental, or evolutionary studies where stromatoporoids play a key role as biostratigraphic and palaeoecological indicators. In museums, it can assist in cataloguing and curating under-identified material, especially in collections where specialist expertise is scarce. For education, the system provides an interactive learning tool, supporting student training in fossil recognition and taxonomic principles, enhancing their understanding of fossil morphology and taxonomy through interactive, AI-supported feedback. Furthermore, by enabling more efficient digitization and classification of thin section imagery, the project supports broader efforts in digital heritage preservation and open-access paleontological databases. Ultimately, this AI framework may be expanded to include other fossil groups with complex skeletal architectures, positioning it as a versatile model for automated identification in palaeontology.

Materials and methods

Four stromatoporoid taxa from a single assemblage in the upper Wenlock (middle Silurian) strata of the Much Wenlock Limestone Formation, located in the English Midlands, were selected for this study (Figure 1).

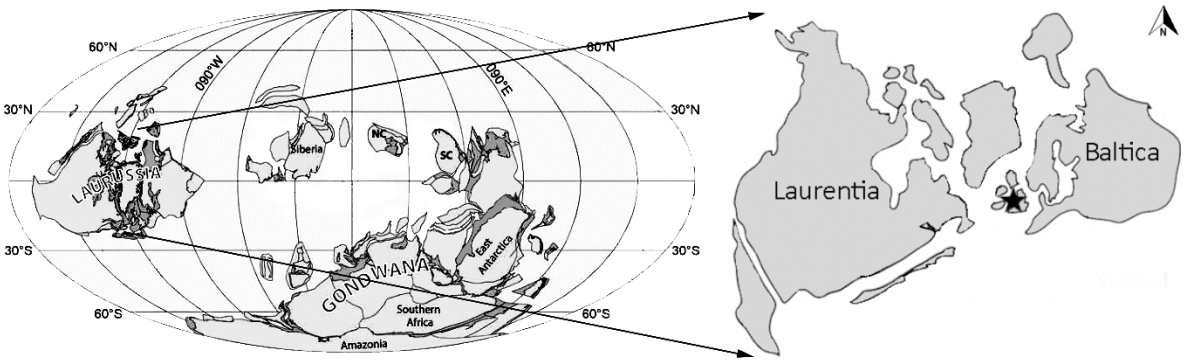

Figure 1. Palaeogeographic map of the Middle Silurian, showing the location of the English Midlands (indicated by star) (after Torsvik and Cocks, 2016).

These samples were selected due to their well-preserved skeletal features and are part of a focused study in a monograph where their taxonomy was studied in detail in vertical and transverse thin sections (Kershaw et al. 2021). All the material used in this study was collected from outcrops in Shropshire and the West Midlands of the Much Wenlock Limestone Formation, upper Wenlock, Silurian. Figure 2 illustrates examples of stromatoporoids in field and hand specimen views.

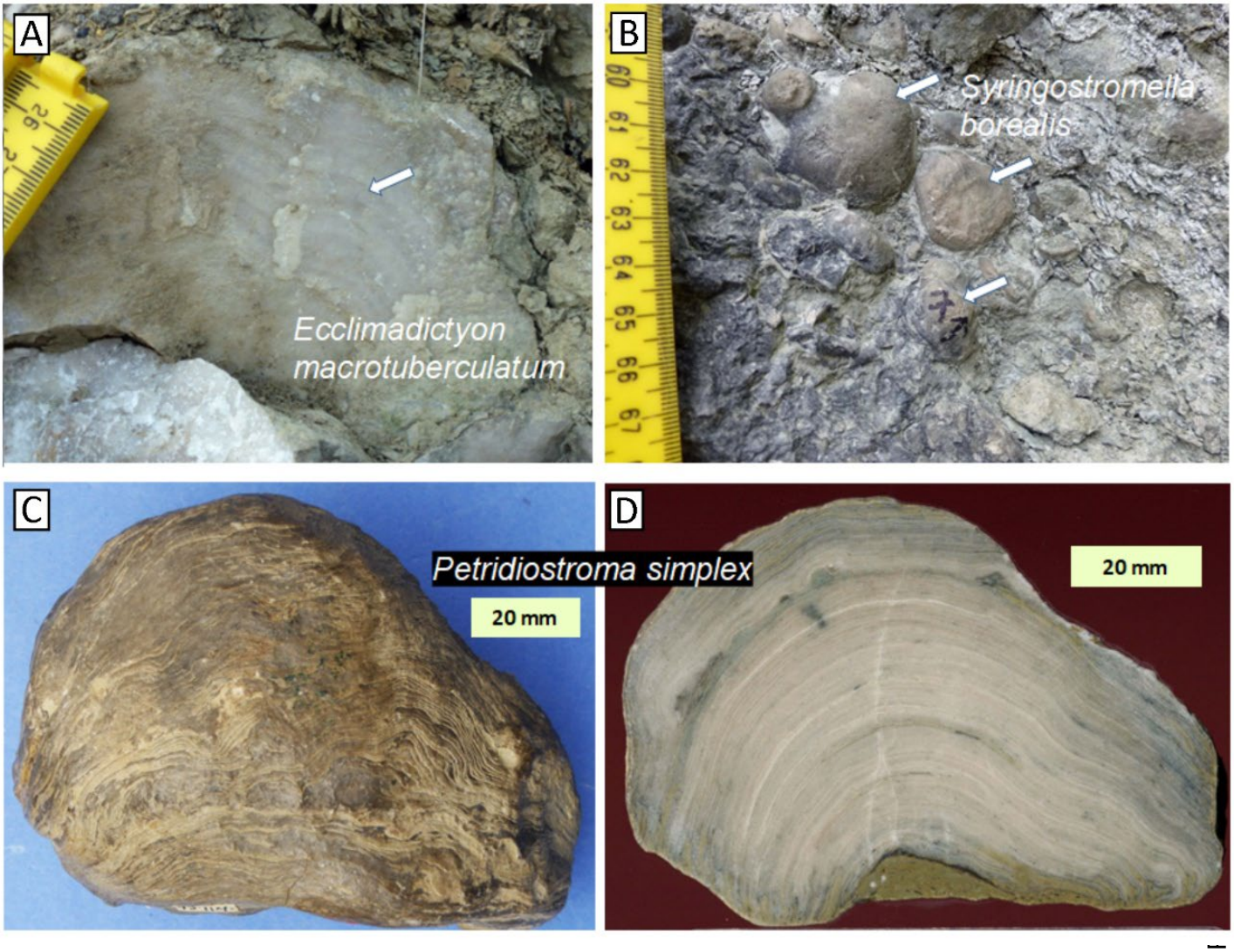

Figure 2. **A**. Field view of stromatoporoid taxon *Ecclimadictyon macrotuberculatum*, broken open on the rock face to reveal a vertical section through the fossil. Its layered character is shown by the banding (arrow). This stromatoporoid sits on another fossil, lower left, and is overlain by a mixture of soft muddy carbonate sediment with fossil fragments. Coates Quarry, Wenlock Edge, Shropshire. **B.** Field view of several apparently subspherical stromatoporoids of the taxon *Syringostromella borealis* (arrowed), in a layer in muddy carbonate sediment. Wrens Nest, Dudley, West Midlands. **C, D.** External surface (C) and vertically-cut polished surface (D) of stromatoporoid *Petridiostroma simplex*, showing its prominent layered structure. Wrens Nest, Dudley, West Midlands, sample 93-117 of National Museum of Wales, Cardiff, see Kershaw et al. (2021) for permissions.

Figure 3 shows cut blocks, sawn with faces at 90 degrees, to demonstrate the relationships between vertical and transverse appearances of the skeletal structure of stromatoporoids, important for the AI analysis and classification.

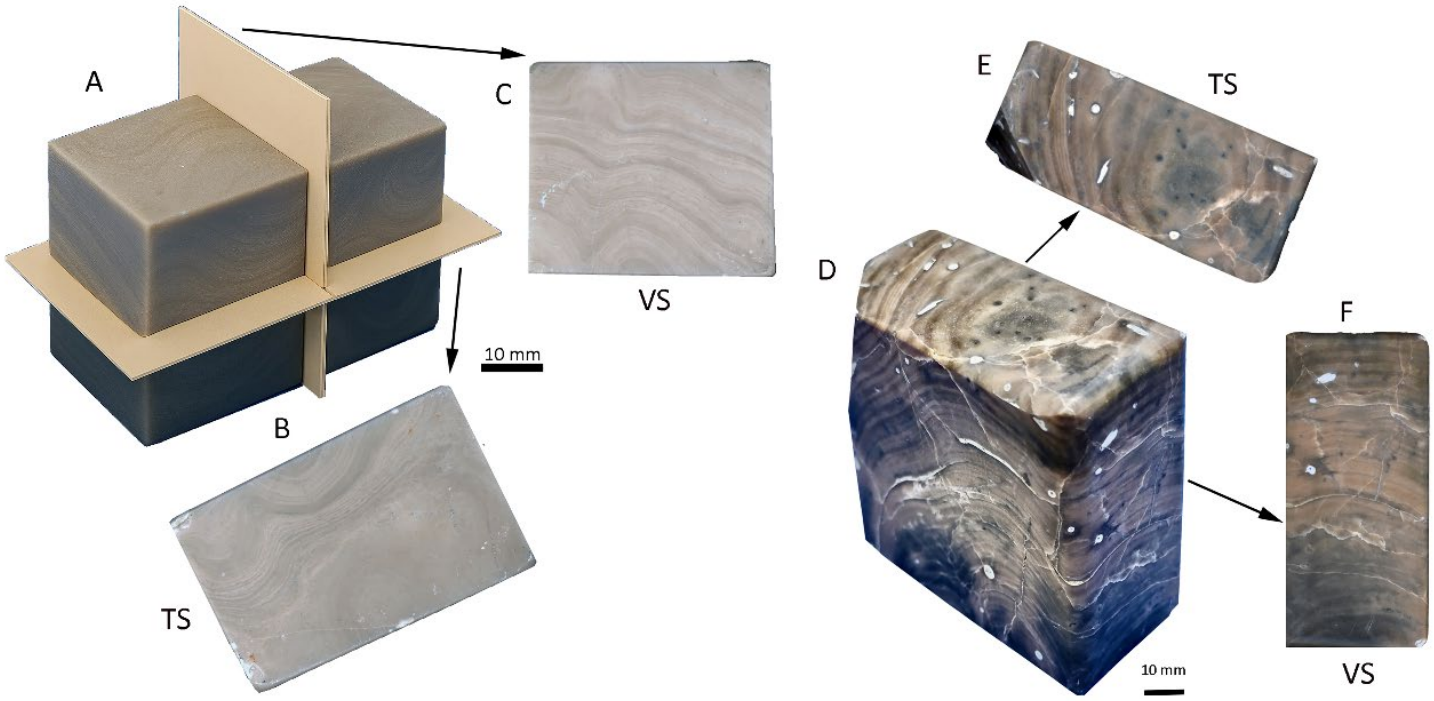

Figure 3. 3D stromatoporid samples that were cut into blocks showing vertical (VS) and transverse (TS) sections of the orientations used to make thin sections. A: whole block of stromatoporoid with cut lines at 90 degrees, indicating the orientations used to make thin sections; B show TS and C shows VS planes. D: whole block of another specimen in three dimensions; E shows the top of the block for the TS view, and F shows the side of the block for VS view.

Figure 4 shows major features of stromatoporoid architecture in thin sections, that the AI system analyses to develop an identification system.

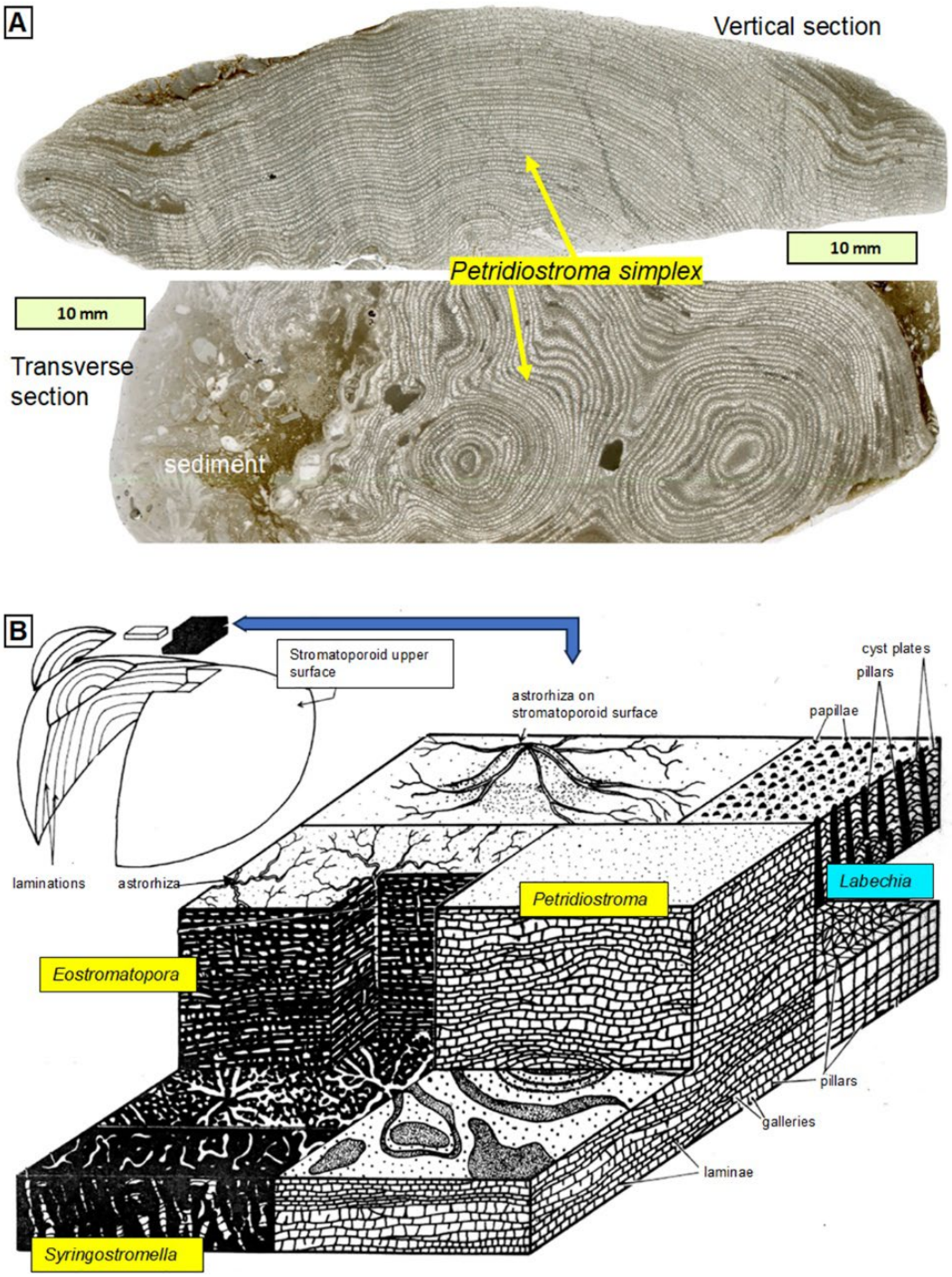

Figure 4. **A.** Vertical section [VS] and transverse section [TS] whole-thin-section scans of *Petridiostroma simplex*. Stromatoporoid taxonomy is studied using a combination of the VS and TS views, applied in this study to develop an AI model. The VS view, in this particular specimen, shows somewhat wavy laminae and intervening pillars; the TS view shows individual pillars in transverse section, and also the laminae are slightly obliquely sectioned, so they are visible in this view. The fossil is embedded in sediment made of muddy carbonate and small shell fragments.
B. A schematic three-dimensional diagram showing a domical-shaped stromatoporoid, upper left, cut vertically and horizontally to reveal its general internal lamination. The opaque irregular block is enlarged in the main diagram to show four examples of stromatoporoid skeletal architecture, three of which, highlighted in yellow, are used in this study. These architectures are not present in one individual real stromatoporoid fossil, instead they represent different species, but are shown together here to emphasise the contrasts between species. Thus, note the significantly different arrangements of the architecture, critical for the identification and thus for the AI approach. The fourth, highlighted in blue, is very different from the others, and is characterised by curved plates and stout vertical pillars, representing a species that is not used in this study. This diagram thus demonstrates the wide variety of structure in stromatoporoids, thus only part of that variation is addressed in this study.

Figure 5 completes this brief survey of critical aspects of stromatoporoid structure by detailing the vertical and transverse views of all four taxa used in this study.

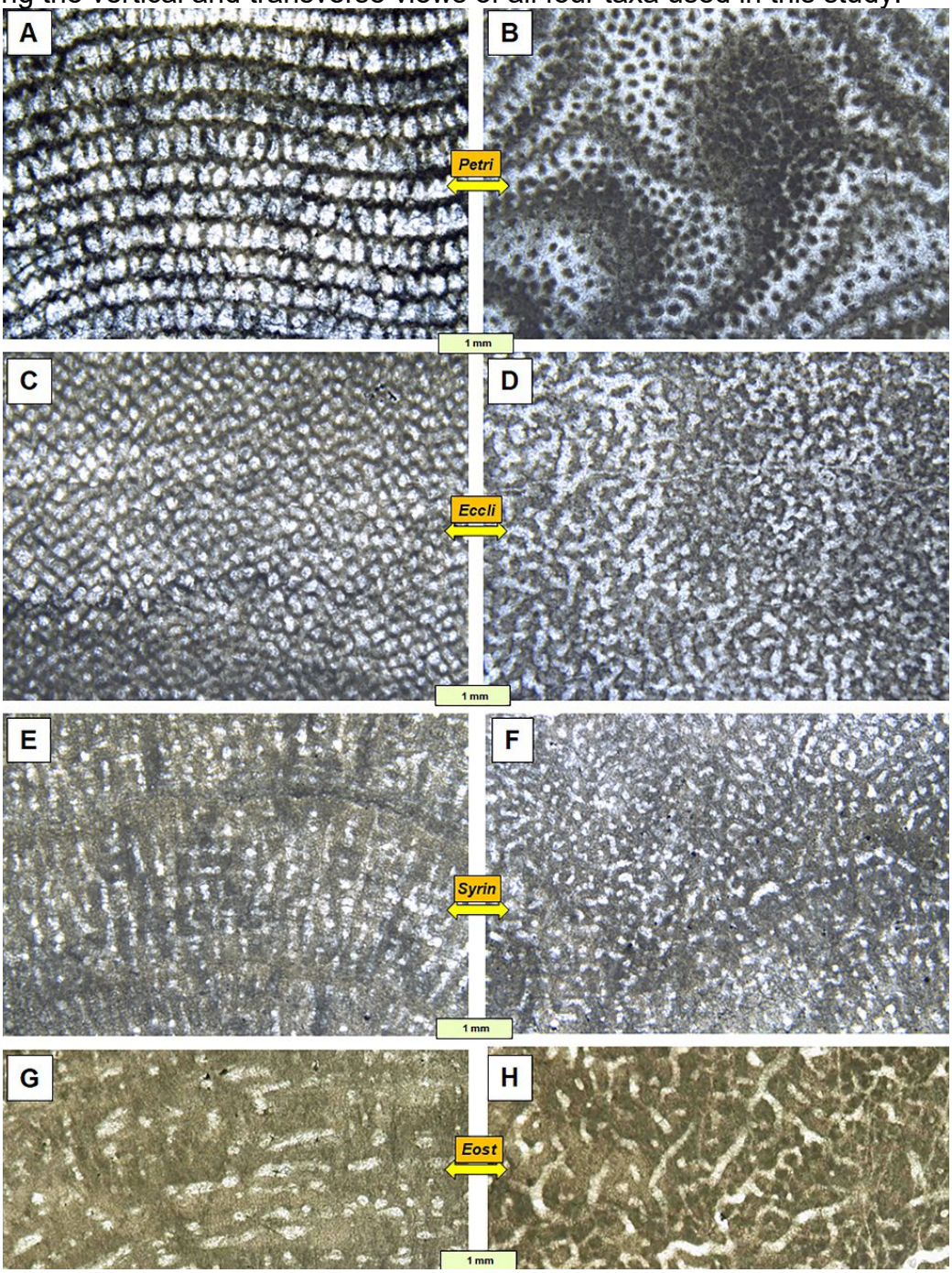

Figure 5. Details of vertical section [VS] (left photos) and transverse section [TS] (right photos) of the four taxa studied here; all photos are at the same scale. **A, B.** *Petridiostroma simplex*, abbreviated to *Petri*, showing its nearly planar laminae, and pillars that are orientated more-or-less normal to the laminae. Pillars are shown as dark dots in the TS view. **C. D.** *Ecclimadictyon macrotuberculatum* (*Eccli*), characterised by a zig-zag architecture in VS view, thus being composed of laminae but almost completely lacking pillars. The TS view (D) indicates the ridges and troughs of the zig-zags comprise short lengths arranged without any preferred orientation. **E.F.** *Syringostromella borealis* (*Syrin*) typified by prominent thick vertical elements with less occurrence of thick horizontal elements; however in the intervening clear spaces are abundant thin plates, called dissepiments, that connect the vertical elements. In TS (F) the vertical elements are shown to have a complex boxwork structure, enclosing the same clear spaces as seen in E. **G, H.** *Eostromatopora impexa* (*Eost*), comprising thick vertical and horizontal elements, seen in VS (G), with some thin dissepiment plates in the clear spaces between the elements. The TS view (H) reveals the skeletal elements comprise a complex mass of dark skeletal material enclosing clear spaces that vary from small circles to elongate wavy channels (the latter are part of the excurrent flow system of the sponge animal when it was alive).

A total of 993 images were used in this study (see Table 1 for their distribution and additional material for comprehensive specimen data), including both vertical and transverse sections. Although the sample set seems to consist of a low number of thin sections (Figures 3-5 illustrate the VS and TS specimen views), compared to other AI studies, it is adequate for taxonomic study of stromatoporoid fossils because the variation within these taxa in this sample set is not sufficiently large to cause problems of classification. Nevertheless, other stromatoporoids, not studied here, do have strongly variable structure, and emphasise that this study is an initial approach, that can be developed across all stromatoporoid taxa in future.

Taxon	**Number of individuals**	**Number of images**	**Breakdown**
Ecclimadictyon macrotuberculatum	16	158	154 images of individuals with TS & VS 4 images of individuals with only VS (2 individuals)
Petridiostroma simplex	8	114	82 images of individuals with TS & VS 32 images of individuals with only VS (9 individuals)
Eostromatopora impexa	7	211	193 images of individuals with TS & VS 8 images of individuals with only TS (1 individual) 10 images of individuals with only VS (1 individual)
Syringostromella borealis	12	510	504 images of individuals with TS & VS 6 images of individuals with only VS (1 individual)
Total	**43**	**993**	933 images of TS & VS, 60 images of VS or TS

Table 1. Image distribution by taxon and section type. TS = transverse section; VS = vertical section

The collection and identification of fossil stromatoporoids present several challenges that directly impact the development of an AI-based classification system. Fossil specimens are often difficult to access, as their discovery depends on targeted field campaigns in regions that may require special permits for collection. Once obtained, the samples must be processed and transported to a laboratory for analysis. Taxonomic identification is further complicated by the fact that specimens initially thought to be stromatoporoids in the field are sometimes later found to be other fossils, e.g. corals, necessitating the preparation of thin sections to confirm their identity, an effort that increases both time and cost. Moreover, the production of thin sections is significantly expensive, adding another layer of difficulty to the overall process. These constraints underscore the value of developing automated classification tools to streamline and standardize the identification process.

Dataset Description

The dataset used in this study reflects the realities of fossil collection and curation over many years, with specimens gathered between 1980's and 2015 from several field visits across Silurian outcrops in central England; these were supplemented by study of museum collections. Samples vary in size and number for each species, controlled by variation in their occurrence and accessibility in outcrops; this variation exists because stromatoporoids vary in size and abundance in the limestones in which they occur. Stromatoporoids vary in size from a few mm to 1 m or more, yet each one represents an individual organism, regardless of how small or large they are. Specimens of a few mm size are not amenable for machine learning training because they lack the scale of growth development needed. Thus, specimens of minimum of a few cm size were used for the training process, although some were 20 cm or more in size in the training set. The result is a lack of standardization in the number of thin sections per species, as well as in the types and quality of photographic documentation. This variability stands in contrast to the large uniform datasets often used in machine learning applications. Moreover, fossil preservation introduces further constraints: specimens must not only be abundant but also well-preserved and structurally suitable for thin-sectioning, with clearly visible diagnostic features. A problematic character of stromatoporoids is that their preservation varies, leading to variation in appearance in thin sections; some, which are too poorly preserved to be identifiable, were of course excluded from this study. These limitations restrict the degree of standardization achievable in the dataset and present unique challenges for automated image analysis.

The reason for choice of the particular taxa used in this study is because of the high number of thin sections already prepared from these taxa, which are abundant in the target rock formations. These taxa are well-established and were used in a monograph work on British Silurian stromatoporoids by Kershaw (SK), Sendino (CS) and Da Silva (ACDS) (Kershaw et al. 2021). The material comprises a combination of a) original field samples collected by Kershaw (SK) and Da Silva (ACDS), and samples loaned by the National Museum of Wales, Cardiff, from which new thin sections were made; and b) existing thin sections from historical collections held by the Natural History Museum, London (facilitated by CS), and the Sedgwick Museum, Cambridge, England. The original field samples collected by SK and ACDS are deposited in the Sedgwick Museum, Cambridge, England. Photomicrographs of the thin sections, originally produced for the monograph, were used in this study. The fossils come from a limited range of reef facies and bedded argillaceous limestones in a relatively small area on the western margin of the Midlands Craton in central England, bordering the Welsh Basin to the west. This assemblage likely occupied a consistent shallow marine environment under tropical to subtropical conditions when the UK was positioned in low latitudes (see palaeogeographic and stratigraphic details in Kershaw et al., 2021).

For analytical purposes, the four stromatoporoid taxa were grouped into two morphological groups for analysis, based on their broad similarity within each group:
Group A: *Petridiostroma simplex* and *Ecclimadictyon macrotuberculatum*, both characterized by thin, extensive horizontal laminations with interspersed vertical to subvertical elements.
Group B: *Stromatopora impexa* and *Syringostromella borealis*, both of which have thick vertical structural elements and some variability in horizontal orientations.

This grouping was design to test whether the AI algorithm can reliably distinguish between taxa with broadly similar internal architectures, as a way of groundtruthing the application of the algorithm. Beyond morphological categorization, this

grouping also served a functional role in evaluating the AI model's classification capabilities. By testing the model on both intra-group (similar architecture) and inter-group (distinct architecture) comparisons, we assessed its sensitivity to subtle structural differences and its robustness in distinguishing taxa with overlapping features. This approach provides insight into the model's ability to generalize across varying degrees of morphological similarity, a critical factor for future applications in automated fossil identification.

Thin sections were photographed in transmitted light in an optical microscope and the resulting digital images were enhanced as they would be for publication in a taxonomically focused paper. These final images were then scanned and processed to identify the elements for AI analysis.

Image Preprocessing

To prepare the dataset for training and evaluation, all thin section images underwent a standardized preprocessing workflow designed to enhance model performance while preserving the identifying features of stromatoporoid skeletal architecture, as explained below.

Manual Preparation and Format Conversion

Initially, images were manually cropped to isolate regions of interest containing fossil structures and avoid empty areas in the thin sections. This ensured that irrelevant background material was excluded, focusing the model's attention on the skeletal features critical for taxonomic identification. Original image formats included both TIFF and JPG; all images were converted to JPG to maintain consistency and reduce file size, facilitating efficient processing.

Creation of training, validation and test sets

As stated above our approach is based on the development of a machine learning model that takes as input a pair of images (TS and VS) corresponding to the same specimen. In order to prepare adequate training, validation and tests sets we start from the 933 images corresponding to individuals with both TS & VS images.
From these, we created a list of all the possible pairs of images one TS and one VS for an individual that are a total of 7216 pairs. Next, we divided these in training, validation and test subsets, taking care that no individual was present in more than one set, while trying to balance the presence of each species in each of the subsets, this probed to be challenging given the scarce number of samples for some of them. We then created CSV files for each of these sets to ensure reproducibility.

Preprocessing Pipeline

Subsequent preprocessing (in the training script) was implemented using the *torchvision.transforms* module in PyTorch [Ansel et al., 2024]. The following transformations were applied:

- Resizing: All images were resized to 224 × 224 pixels to ensure uniform input dimensions compatible with the convolutional neural network (CNN) architecture.
- Data Augmentation (Training Set Only): To improve generalization and reduce overfitting, the training dataset was augmented with:
    - Random horizontal flips
    - Random rotations up to ±15°

- Image brightness, contrast, saturation, and hue adjustments.
- Image normalisation with values in the [0,1] range.

For the validation and test sets, the same resizing, and normalisation steps were applied, but without any data augmentation, ensuring an unbiased evaluation of the model's performance on unseen data.

Data Loading

To efficiently train and evaluate the machine learning model, the data were loaded in small groups or batches of 16 samples at a time, enabling efficient mini-batch training and evaluation. A custom Python class was implemented to handle the loading of paired vertical and transverse view images along with their corresponding labels. This class parsed the structured CSV files generated before, ensuring that each sample included both orientations required for accurate taxonomic classification.

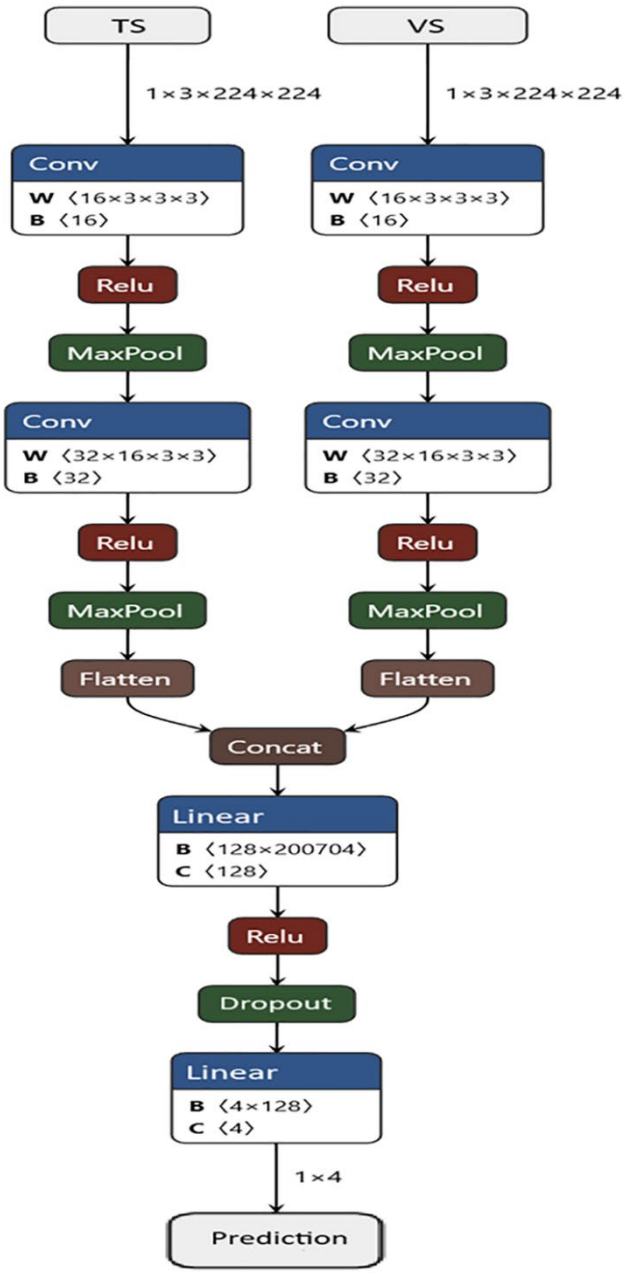

ANN (Artificial Neural Network) Architecture

The classification model employed in this study was a custom-designed CNN specifically tailored to process paired image inputs representing the vertical and transverse views of stromatoporoid thin sections (Figure 6). The model architecture consists of two parallel convolutional streams—one for each image orientation. Each stream was designed to independently extract spatial features from its respective view, enabling the model to learn complementary patterns. We will refer to this model as DualStreamsCNN (Table 2).

Figure 6. Diagram of the CNN architecture used in this study. The figure illustrates the flow of gradients through the network's layers, including convolutional layers, ReLU activations, max-pooling operations, and fully connected layers. Weight and bias tensors are annotated with their respective dimensions (e.g., top_conv1.weight [16, 3, 3, 3], fc1.weight [128 × 20976]). Gradient accumulation and layer-specific backward operations, e.g., ConvolutionBackward0, ReLUBackward0, MaxPool2DWithIndicesBackward0) are shown, culminating in the final output gradient (c_1:4). This architecture supports feature extraction and classification tasks, such as fossil recognition.

Taxon	Precision	Recall	F1-score	Support
Ecclimadictyon	0.72	0.99	0.83	124
Eostromatopora	0.95	0.62	0.75	262
Petridiostroma	0.00	0.00	0.00	26
Syringostromella	0.92	0.98	0.95	1103

Table 2. DualStreamsCNN overall Classification Report

Each stream included:

- Two convolutional layers:
  - First layer: 3 input channels (RGB), 16 output channels, kernel size of 3×3, padding of 1, followed by a ReLU (Rectified Linear Unit) activation.
  - Second layer: 16 input channels, 32 output channels, kernel size of 3×3, padding of 1, followed by a ReLU activation.
- Max-pooling layers followed each convolutional layer, with a kernel size of 2×2 and a stride of 2, effectively reducing the spatial dimensions by a factor of 4 across the two layers.

The output feature maps from the final pooling layers of both streams were flattened and concatenated along the feature dimension, forming a unified representation of both views. This resulting feature vector was passed through a fully connected classification head comprising:

- A fully connected layer with 200,704 input features and 128 output features, followed by a ReLU activation.
- A dropout layer with a dropout probability of 0.5 to reduce overfitting.
- A final fully connected layer with 128 input features and 4 output features, corresponding to the four taxa.

This model architecture was designed to leverage the complementary information present in both orientations, mimicking the dual-view approach traditionally used by taxonomists. In our initial experiments, we had data from only two of the taxa (*Eostromatopora impexa* and *Petridiostroma simplex*) with a limited number of individuals (see Table 1). We also developed a single view (used for TS and VS) training model to compare with our dual stream model, to check if there was improvement, and we observed a great improvement over the 50 and 55% accuracy observed for single TS and VS models. However, for the full dataset with the addition of the two new taxa, the model struggles with the underrepresented taxa (*Eostromatopora impexa* and *Petridiostroma simplex*).

In view of this, for further experiments, we developed a new model based on a pre-trained RESNET-50 network (see Kaiming He, 2016) for feature extraction with transfer learning, initialised with the IMAGENET1K_V1 weights. This was configured as a Siamese network taking as inputs again a TS and a VS from an individual. The purpose is to evaluate the impact of transfer learning. We will refer to this network from here on as the DualResNet.

Training Process

The models were trained end-to-end using the AdamW optimizer with a learning rate of 0.0003. The training objective was to minimize the cross-entropy loss, which quantifies the difference between the predicted class probabilities and the true class labels. To address the class imbalance that is present in the training dataset, a weighted cross-entropy loss function was employed. Class weights were computed based on the inverse frequency of each class in the training set, thereby assigning greater importance to underrepresented taxa and encouraging the model to learn from minority class examples more effectively.

After each epoch, each model's performance was evaluated on the validation set to monitor generalization and detect signs of overfitting. No explicit hyperparameter tuning was conducted beyond the initial configuration. Upon completion of training, for which we used early stopping tracking the validation loss, they were evaluated on a separate test set consisting on 1515 image pairs that had not been used during the machine training or validation. Each pair consisting of VS and TS images of the same specimen. The evaluation in both cases was conducted without any data augmentation to ensure an unbiased assessment of the model's performance. The following metrics were computed: overall accuracy, precision, recall, and F1-score, we also generated a confusion matrix to show class-specific performance and misclassification patterns.

Results

The models were trained using a weighted cross-entropy loss function to mitigate the effects of the observed class imbalance in the training dataset. This weighting strategy aimed to provide greater emphasis to the under-represented classes during the learning process.

DualStreamsCNN

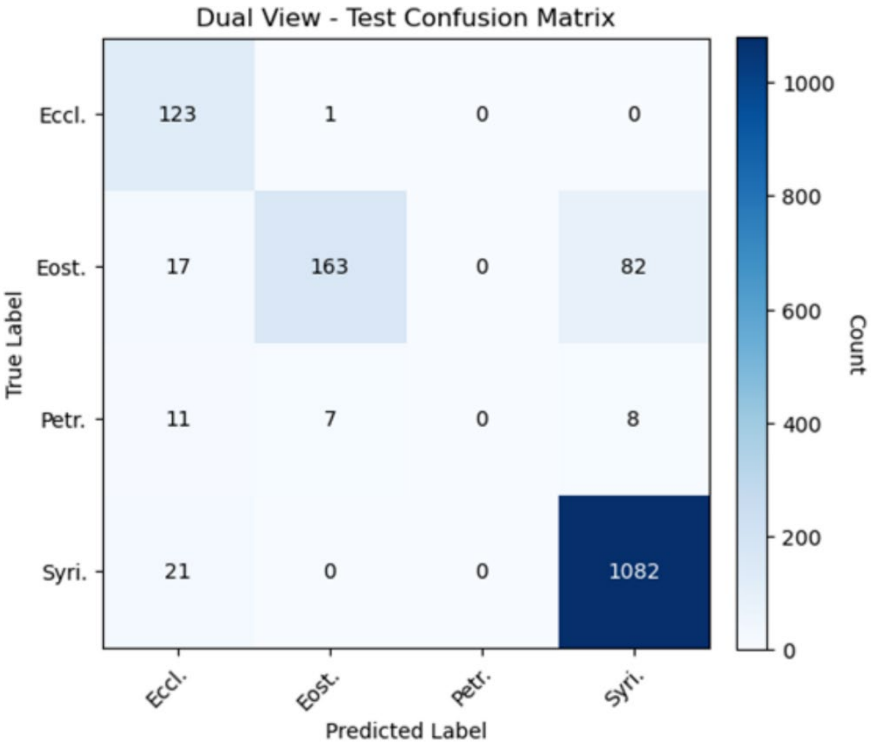

We obtained an accuracy of 90.30% across all image pairs (n=1515) in the test subset. To further evaluate the model's ability to generalize to each individual object class, per-class accuracy was assessed (Table 2). The results are presented in the confusion matrix show in Figure 7.

Figure 7. Confusion matrix obtained with the DualStreamsCNN model across the four taxa studied: Eccli. =Ecclimadictyon; Eost. = Eostromatopora; Petri. = Petridiostroma; and Syrin = Syringostromella. The correct classifications are located in the main diagonal.

The model performs very well overall, but even with the weighted classes mechanism it clearly struggles with the less represented classes especially with the *Petridiostroma*. The overall classification report provides a more detailed breakdown of the model's performance, including precision, recall, and F1-score for each taxon, shown in Table 3.

DualResNet

On the other hand, the DualResNet avoids some of these problems, and it improves the overall accuracy to 96.96%. In particular it improves the handling of the minority taxa, although there is still room for improvement. See detailed metrics in Table 3 and Figure 8.

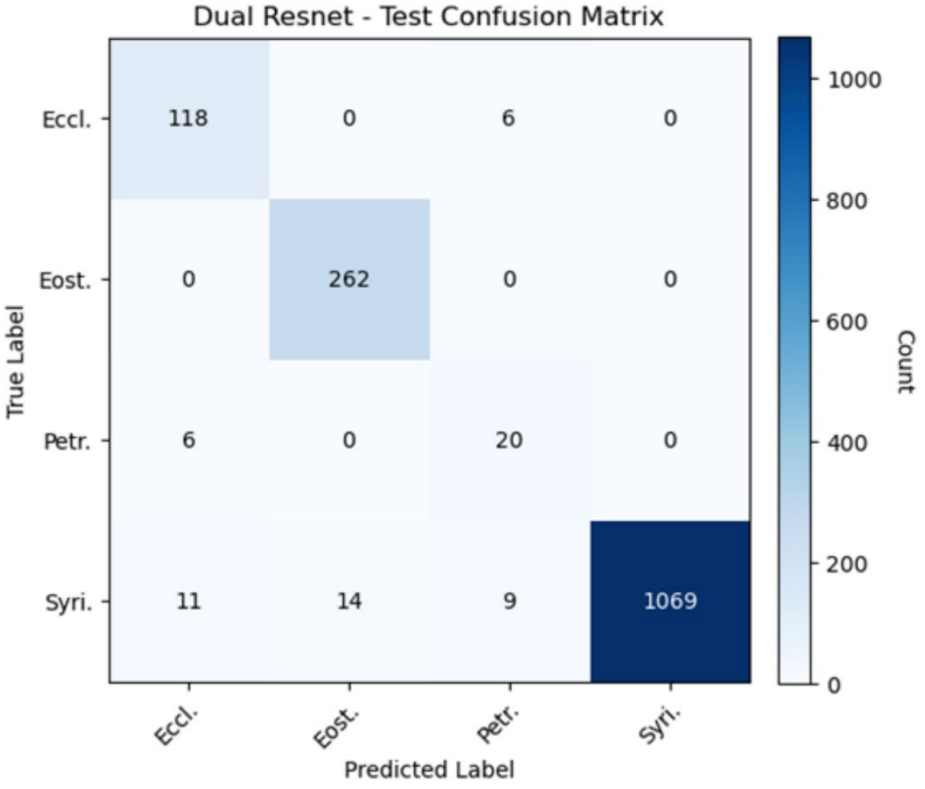

Figure 8. Confusion matrix obtained with the DualResNet model across the four taxa studied. Note the high accuracy of identification of the taxa, and the small number of datapoints where identification was incorrect.

Taxon	**Precision**	**Recall**	**F1-score**	**Support**
Ecclimadictyon	0.87	0.95	0.91	124
Eostromatopora	0.95	1.00	0.97	262
Petridiostroma	0.57	0.77	0.66	26
Syringostromella	1.00	0.97	0.98	1103

Table 3. DualResNet overall classification report.

Visualisation

In order to get some hints of which part of the images are driving the ANN decisions with have uses the Grad-CAM algorithm (Selvaraju et al. 2019) to generate heatmaps that show in warmer colours the regions of an image that contribute most to the ANN prediction. In Figure 9 we present an example for each of the taxa, including the ANN TS and VS input images, and the TS and VS heatmaps generated using Grad-CAM.

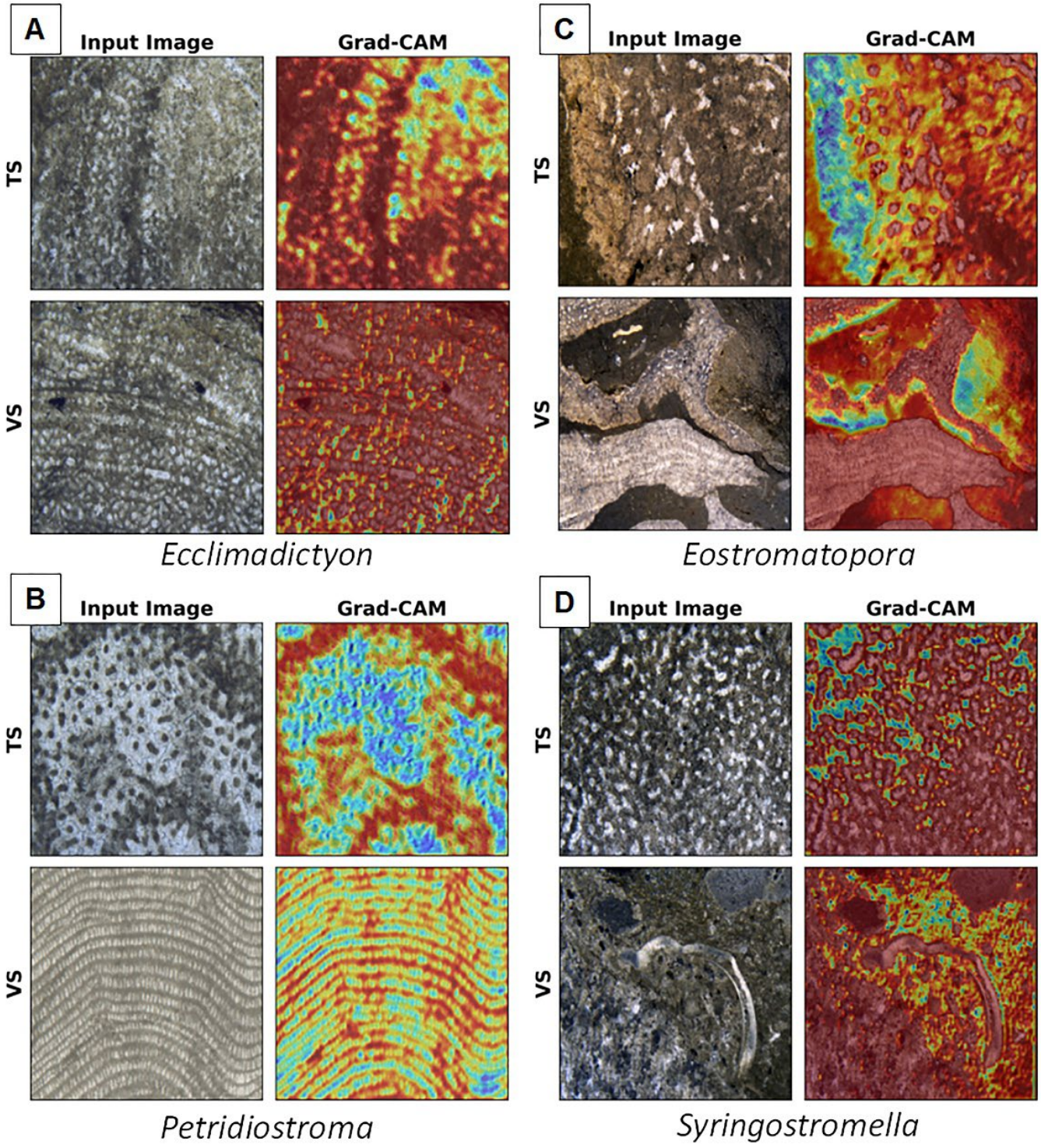

Figure 9. Heatmaps for TS and VS input images. We present one example for each taxon in each subplot (a) to (d). In each subplot, the first row corresponds to the TS orientation with the input image in the first column and the Grad-CAM generated heatmap in the second. The second row shows the images for VS.

Discussion

The high overall accuracy of the models (90.30% and 96.96%) on the test set indicates that the models effectively learned to classify the objects based on the paired vertical and transverse images. This result confirms that the model successfully learned to extract and integrate diagnostic features from both orientations, reflecting the dual-view approach traditionally used in palaeontological taxonomy.

A more detailed view of the results using the confusion matrices and the metrics highlight some difficulties in handling the very marked unbalances among taxa in the dataset. The use of a weighted loss function addressed the class imbalance present in the dataset in an adequate way. This strategy mitigated the problem, and the network was able to handle the under-represented taxa. The use of a Siamese architecture with pretrained weights (RESNET-50) greatly improved the results for Eccli. (72% to 87% precision) and Petri. (0% to 57%), the underrepresented taxa. The F1-score, which balances precision and recall, also demonstrates strong performance, and an improvement for all the taxa. While we explored other possible ways of handling the unbalance like using FocalLoss instead of cross-entropy loss, or a weighted random sampler, didn't improve the results, and in fact impacted negatively the training.

The slower convergence observed during training with the weighted loss function is a common trade-off. By emphasizing the under-represented classes, the model requires more iterations to learn the subtle features that distinguish them from the majority classes. However, the improved confidence in the model's ability to correctly classify all species, as evidenced by the per-class accuracy, justifies this slower convergence.

Conclusions and way forward

1. This preliminary study of the application of AI methods to hypercalcified sponges demonstrates good success of the system to discriminate between well-established taxa. The results highlight the importance of addressing class imbalance in achieving a fair and accurate classification system, particularly when working with naturally uneven fossil assemblages.
2. The overall accuracy achieved confirms that AI can effectively learn and generalize from paired vertical and transverse thin-section images, mirroring the traditional palaeontological approach. This success lays a strong foundation for expanding AI-assisted taxonomy to more complex and variable fossil groups.
3. The problems posed by under-represented taxa, although mitigated by the use of transfer learning, but further research is needed for improving the classification of underrepresented classes. Future work could also explore further data augmentation techniques, specifically targeted at the under-represented classes; investigate more advanced loss weighting strategies to potentially further improve their classification accuracy; or integrate additional imaging modalities, such as SEM to enrich the feature space.
4. The next stage is to explore problematic stromatoporoid taxa that have highly variable structure which overlaps with other taxa, to try to determine whether the system is able to assist the decision-making process of identification. Moreover, expanding the model to include other grades of hypercalcified sponges would enable broader application across palaeontological datasets.
5. Ultimately, this study represents a significant step toward the development of scalable, automated taxonomic workflows in palaeontology. By combining expert knowledge with machine learning, such systems have the potential to accelerate

fossil classification, support museum curation, and enhance educational tools, while preserving the integrity and depth of traditional taxonomic practice.

Acknowledgments
We are grateful to the Natural History Museum, London, and National Museum of Wales, Cardiff, for access to curated materials in this study. We also thank Natural England for access to Wren's Nest, and the managers of quarries on Wenlock edge, for access to samples, permissions for which are noted in Kershaw et al. (2021). All these were previously published in the monograph by Kershaw et al. (2021) and the images re-used in this study. CS acknowledges the CSIC project MOV-TEC-2024-072 for which she visited the IFCA (Institute of Physics of Cantabria) (Santander, Spain), for the AI and automatic identification for stromatoporoids.

Contributions
CS and SK initiated the study. CS processed the images analysed. SK supported the project by providing images of specimen thin sections. DRG and IVR developed an AI-automated framework to identify thin section specimens. All authors contributed to writing the final manuscript.

Declaration of competing interests
The authors declare that they have no financial or personal relationships with individuals or organizations that could inappropriately influence or bias the content of this work.

Funding sources
CS acknowledges the Spanish National Research Council (CSIC) for funding the project MOV-TEC-2024-072.

Declaration of generative AI and AI-assisted technologies in the writing process.
The authors have not used generative AI or AI-assisted technologies in the preparation of this manuscript.

Data linking
Code and models available at: https://github.com/davrodgon/stroma-ai

References

Ansel, J., Yang, E., He, H., Gimelshein, N., Jain, A., Voznesensky, M., Bao, B., Bell, P., Berard, D., Burovski, E., Chauhan, G., Chourdia, A., Constable, W., Desmaison, A., DeVito, Z., Ellison, E., Feng, W., Gong, J., Gschwind, M., Hirsh, B., Huang, S., Kalambarkar, K., Kirsch, L., Lazos, M., Lezcano, M., Liang, Y., Liang, J., Lu, Y., Luk, C., Maher, B., Pan, Y., Puhrsch, C., Reso, M., Saroufim, M., Siraichi, M. Y., Suk, H., Suo, M., Tillet, P., Wang, E., Wang, X., Wen, W., Zhang, S., Zhao, X., Zhou, K., Zou, R., Mathews, A., Chanan, G., Wu, P., & Chintala, S. 2024. PyTorch 2: Faster Machine Learning Through Dynamic Python Bytecode Transformation and Graph Compilation [Conference paper]. 29th ACM International Conference on Architectural Support for Programming Languages and Operating Systems, Volume 2 (ASPLOS '24). https://doi.org/10.1145/3620665.3640366.

Huang, J.Y., Kershaw, S., Liang, K., Li, Y., Qie, W.K. 2024. Revision of Middle Devonian stromatoporoid *Climacostroma* from South China. *Palaeoworld*, 33, 92-104.

He, K., Zhang, X., Ren, S., & Sun, J. 2016. Deep residual learning for image recognition. Proceedings of the IEEE Conference on Computer Vision and Pattern Recognition (CVPR), Las Vegas, NV, USA, June 27–30, 2016, pp. 770–778.

Kershaw, S., Da Silva, A-C., Sendino, C. 2021. British Silurian Stromatoporoids; Faunas, Palaeobiology and Palaeographical Significance. *Monographs of the Palaeontographical Society*, **175**, publication 660. Pages 1-92, Plates 1-22. DOI: 10.1080/02693445.2021.2027157.

Selvaraju, R. R., Cogswell, M., Das, A., Vedantam, R., Parikh, D., & Batra, D. (2019). Grad-CAM: Visual explanations from deep networks via gradient-based localization. International Journal of Computer Vision, 128(2), 336–359. https://doi.org/10.1007/s11263-019-01228-7

Torsvik, T.H., Cocks, L.R.M., 2016. Silurian. In: *Earth History and Palaeogeography*. Cambridge University Press, pp. 124–137. https://doi.org/10.1017/9781316225523.008.

Wolniewicz, P. 2010. Stromatoporoid biometrics using image analysis software: a first order approach. *Computers and Geosciences*, **36**, 550-558.